

Supporting Information

The Kinetic Resolution of Constitutional Isomers: Ester Hydrolysis Outside a Supramolecular Nano-Capsule

Simin Liu, Haiying Gan, Andrew T. Hermann, Steven W. Rick and Bruce C. Gibb
Department of Chemistry, University of New Orleans
New Orleans, LA 70148, USA

Section	Page Number
a) Table of contents	1
b) Experimental section	2
c) NMR Data for the capsular complexes between 1₂ and esters 2-11	3-5
d) ¹ H NMR shifts data ($\Delta\delta$, ppm) for esters 2-6 upon encapsulation within 1₂	6
e) Selected COSY NMR data for encapsulated esters 2-6	7
f) Competition experiments	8
g) ¹ H NMR spectra of selected competition experiments for esters 2-7	9-10
h) Relative binding constants of ester 2-11	11
i) Hydrolysis of the free esters	12
j) Rate constants for the hydrolysis of esters 2-6	13
k) Kinetic resolution of esters in the presence of host 1	14
l) Hydrolysis of individual encapsulated esters 2-6	15
m) Calculation of the rate constants for ester hydrolysis at 100°C	16
n) Fitting for the hydrolysis of encapsulated esters	17-18
o) Spiking the hydrolysis of an encapsulated ester with dodecane	19
p) The complexation of the hydrolysis products to host 1	20
q) Competition experiment between decanoic acid and ester 2	21
r) References	22

Experimental Section

General

All reagents were purchased from Aldrich and were used without purification. Esters **2**, **3** and **6-9** (Figure S1) were purchased from Aldrich Chemical Company. Known esters **4**, **5**, **10** and **11** were synthesized by the reaction of corresponding acyl chloride with the required alcohol. Products were purified by column chromatography. Host **1** was synthesized according to a previously reported procedure.¹ All NMR spectra were recorded on a Varian Inova-500 MHz spectrometer.

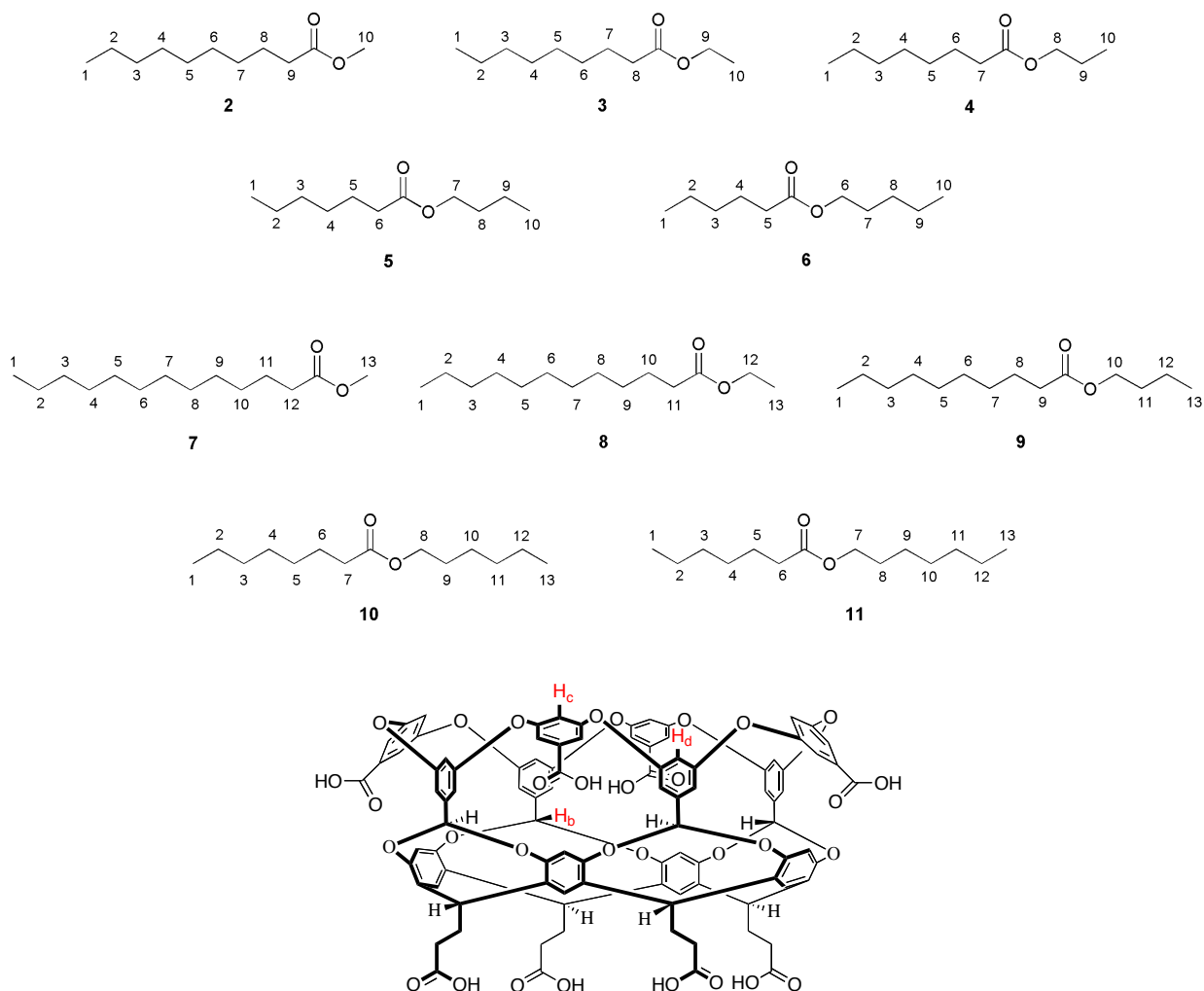


Figure S1: Chemical structures of esters **2-11** and host **1**.

NMR Data for the Capsular Complexes Between **1**₂ and Esters **2-11**

Each titration experiment involved the addition of a concentrated solution (DMSO-d₆) of the guest to an aqueous solution (D₂O) of the capsule **1**₂ (0.5mM in 8.0 mM NaHCO₃). Only the 2:1 capsular complex between **1**₂ and esters **2-11** was observed. The best reporter atoms in the host for confirming guest complexation, protons *b*, *c*, *d* (see Figure S1), are highlighted in each spectrum. COSY NMR experiments were carried to assign all protons.

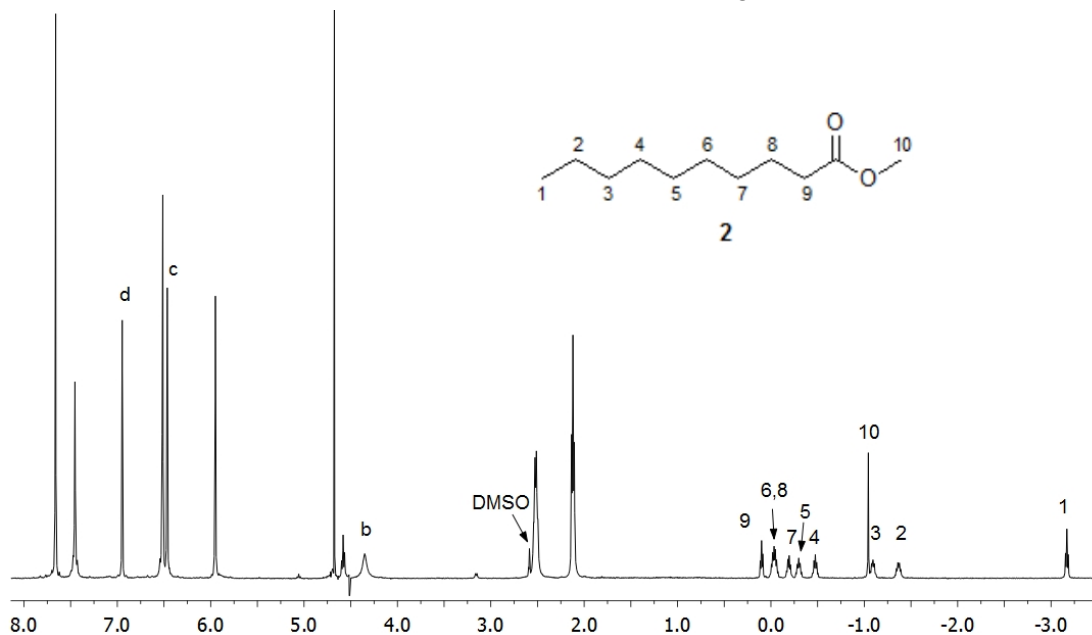


Figure S2: ¹H NMR spectrum of the 2:1 capsule formed between host **1** and ester **2**.

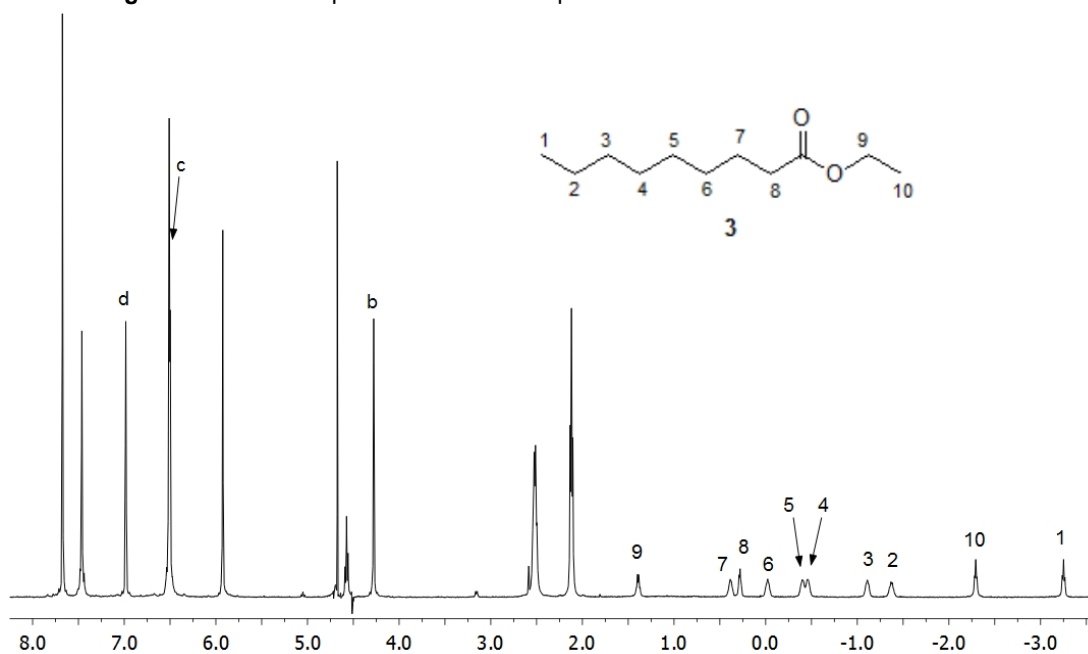


Figure S3: ¹H NMR spectrum of the 2:1 capsule formed between host **1** and ester **3**.

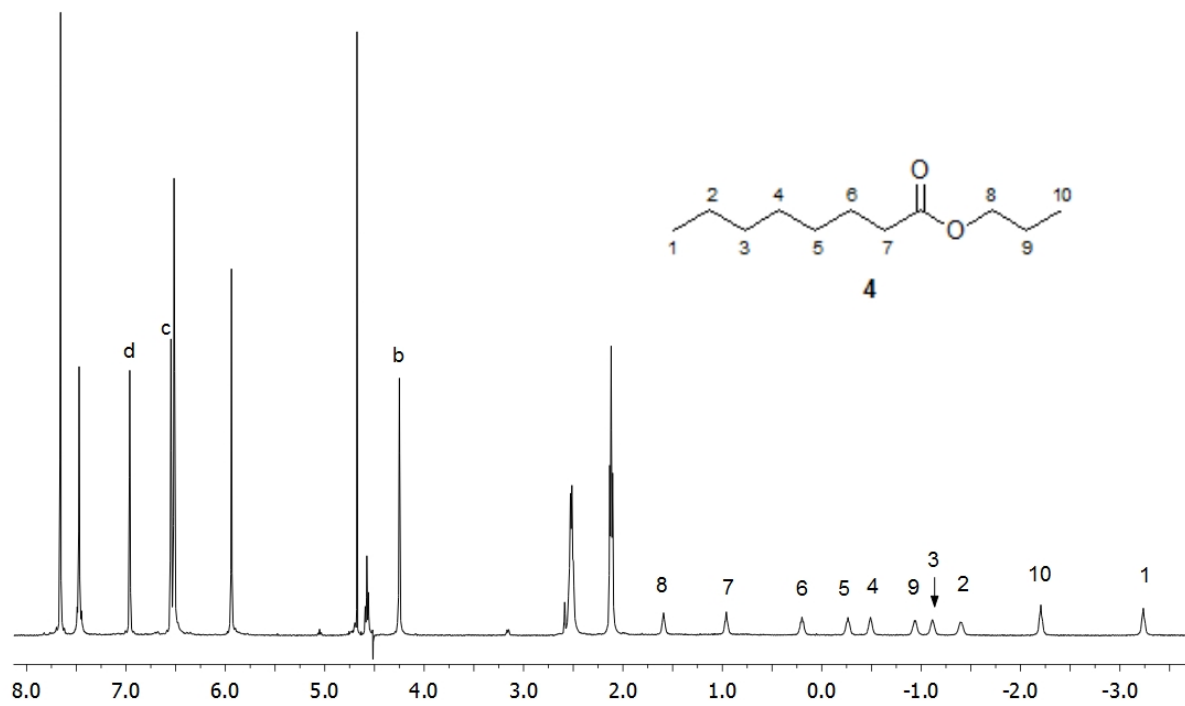


Figure S4: ^1H NMR spectrum of the 2:1 capsule formed between host 1 and ester 4.

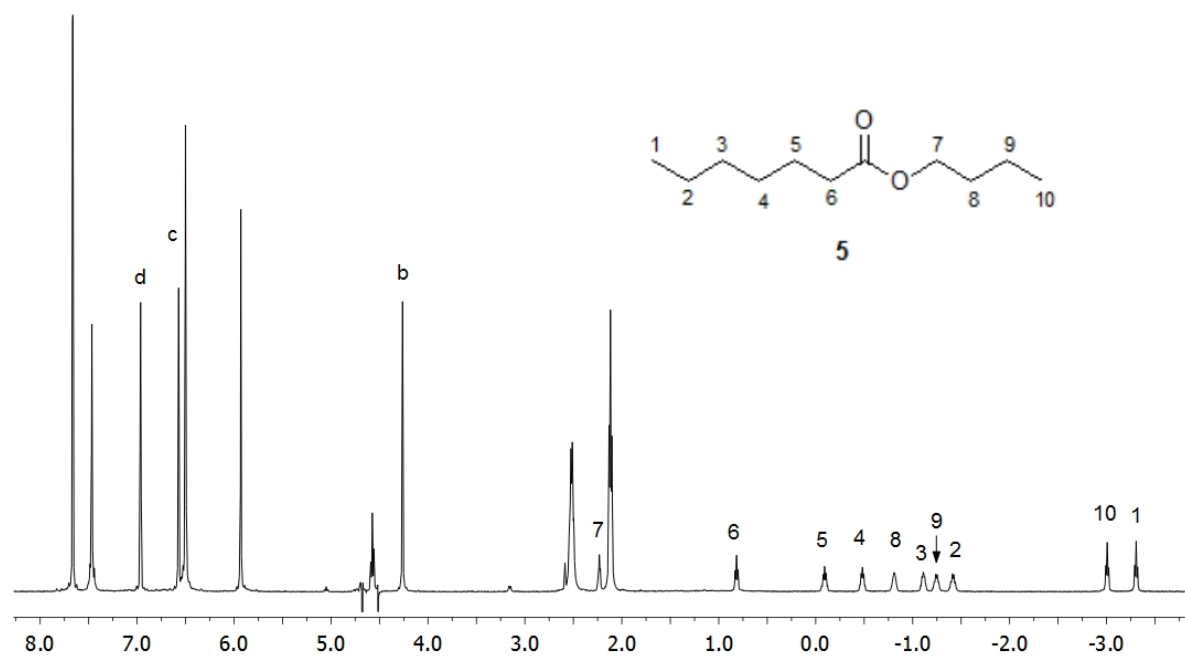


Figure S5: ^1H NMR spectrum of the 2:1 capsule formed between host 1 and ester 5.

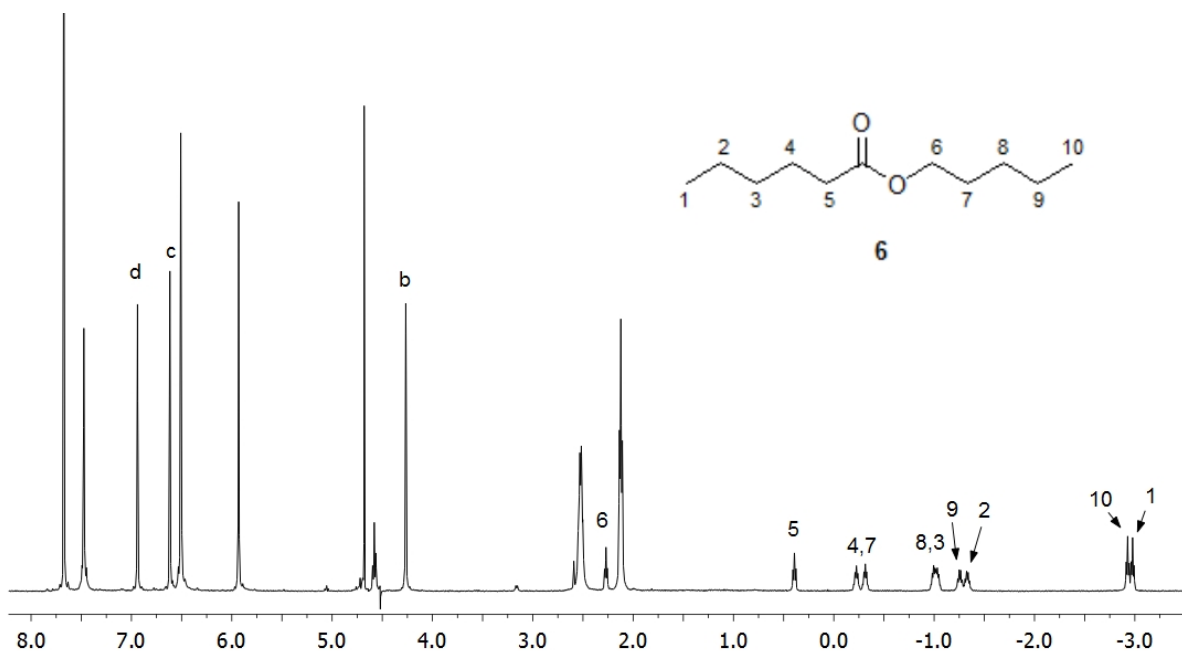


Figure S6: ¹H NMR spectrum of the 2:1 capsule formed between host 1 and ester 6.

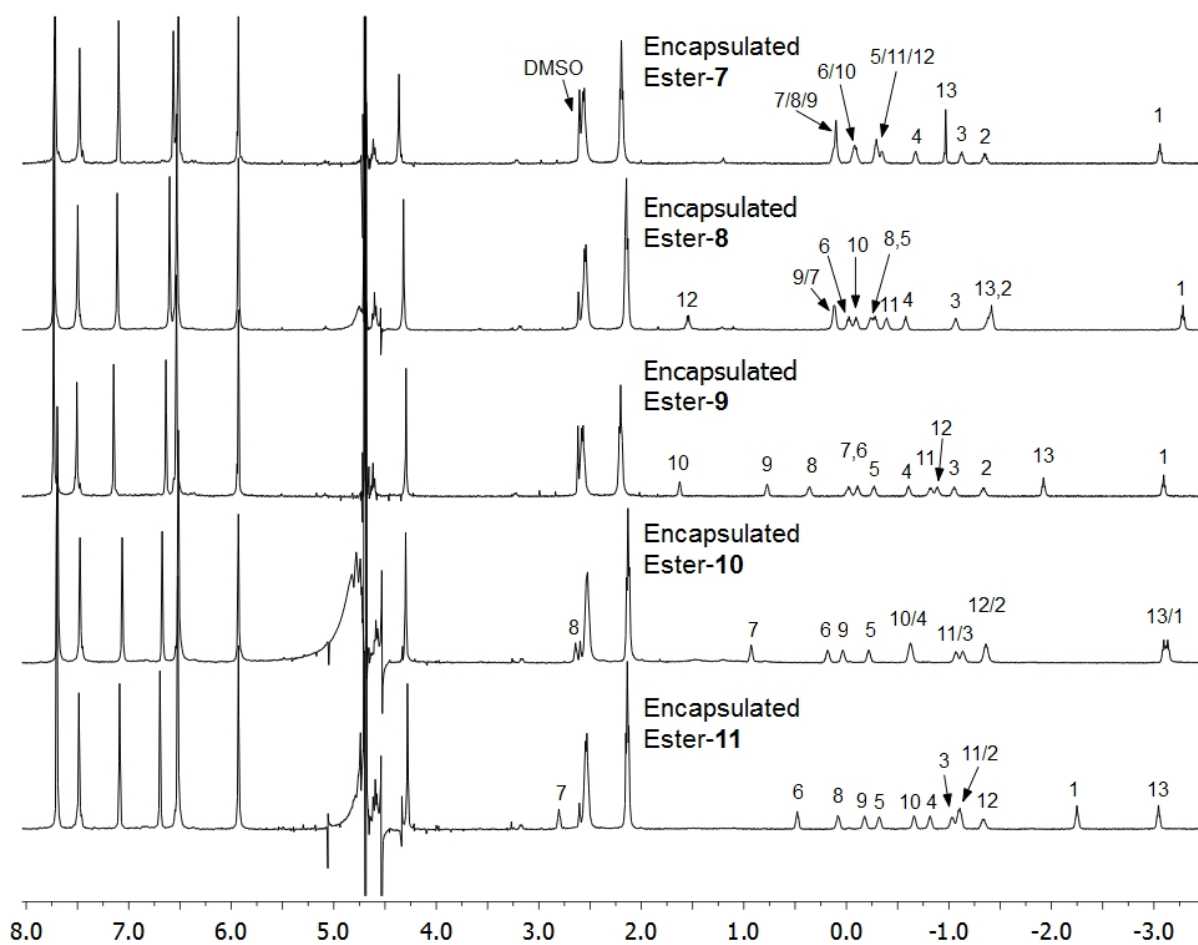


Figure S7: ¹H NMR spectra of the 2:1 capsules formed between host 1 and esters 7-11.

¹H NMR Shift Data ($\Delta\delta$, ppm) for Esters 2-6 upon Encapsulation within **1₂**

All ¹H NMR shift data ($\Delta\delta$, ppm) listed in Table S1 were calculated from the NMR spectrum of the free ester (in D₂O) and the corresponding NMR spectrum of the encapsulated ester. Atom numbering is shown in Figures S2-S6. The data shows that the protons of the two methyl groups (H1 and H10) shifted more than protons located near the center of the ester (methylenes H5, H6 and H7), indicating that a pole-to-pole orientation is the preferred orientation (see Figure 2 in text).

Table S1: ¹H NMR shifts data ($\Delta\delta$, ppm) for esters **2-6** upon encapsulation within **1₂**.

Proton Ester	H1	H2	H3	H4	H5	H6	H7	H8	H9	H10
2	-3.94	-2.55	-2.27	-1.66	-1.48	-1.21	-1.38	-1.52	-2.12	-4.50
3	-4.02	-2.56	-2.30	-1.65	-1.59	-1.21	-1.08	-1.82	-2.55	-3.37
4	-4.01	-2.58	-2.31	-1.68	-1.45	-1.28	-1.15	-2.26	-2.41	-3.00
5	-4.08	-2.60	-2.29	-1.66	-1.55	-1.29	-1.67	-2.27	-2.50	-3.82
6	-3.76	-2.52	-2.24	-1.70	-1.71	-1.62	-1.78	-2.21	-2.45	-3.71

Selected COSY NMR Data for Encapsulated Esters 2-6

Figures S8-S12 show the guest-binding region of the COSY NMR spectra for the encapsulated esters 2-6. Guest protons were assigned according to these spectra.

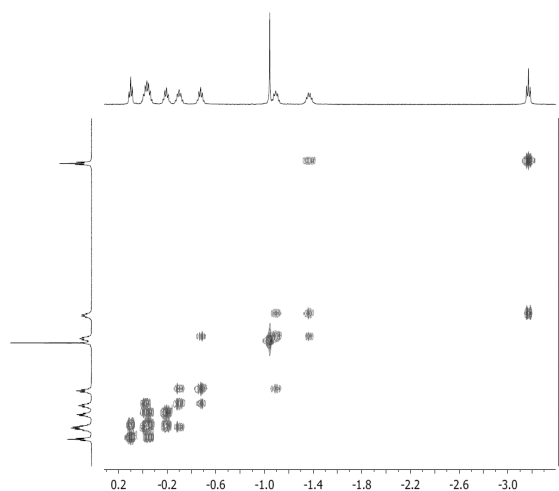


Figure S8: COSY NMR of encapsulated ester-2

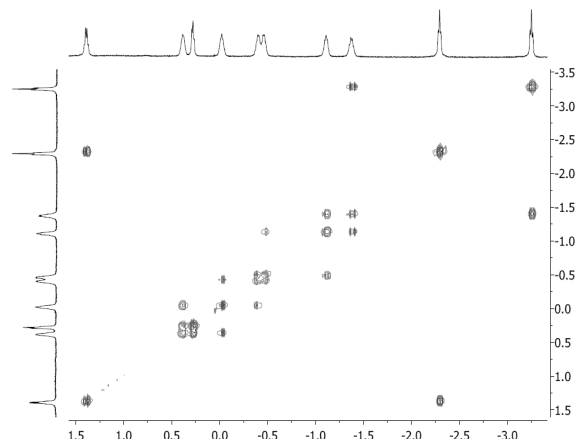


Figure S9: COSY NMR of encapsulated ester-3

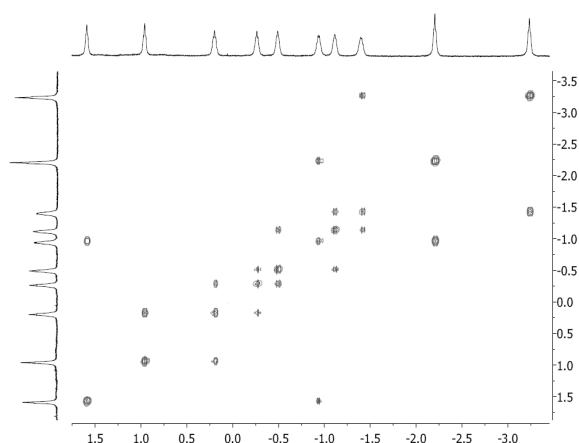


Figure S10: COSY NMR of encapsulated ester-4

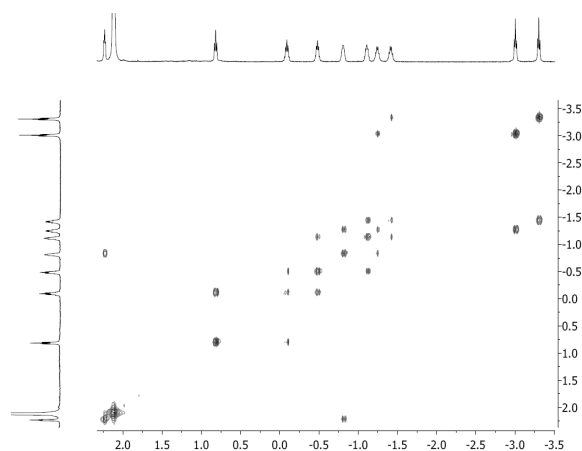


Figure S11: COSY NMR of encapsulated ester-5

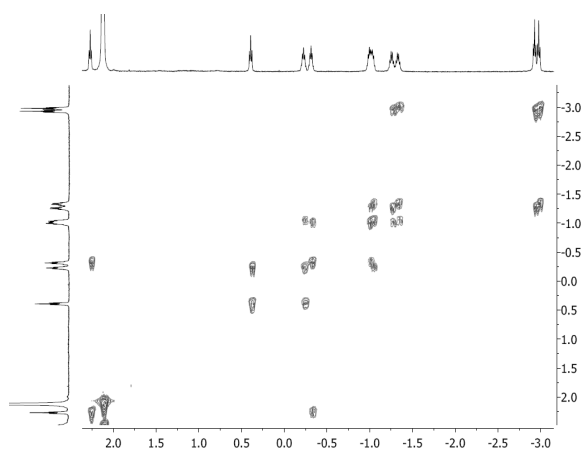
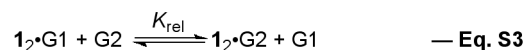


Figure S12: COSY NMR of encapsulated ester-6

Competition Experiments

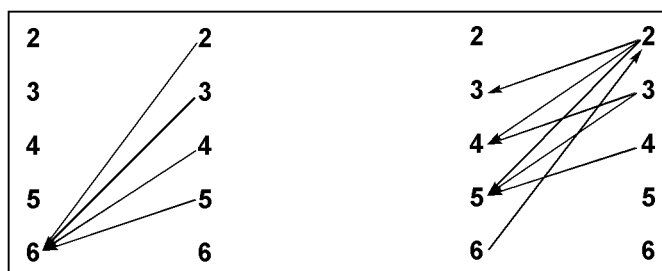
All ^1H NMR competition experiments were performed at 25 °C, with the concentration of host $\mathbf{1}_2$ at 0.5 mM. Spectra were acquired with a long delay time (10 s) to ensure accurate integration. Equations S1–S3 define the thermodynamics of host-guest complex formation for the competition experiments. Equation S4 was used to calculate K_{rel} values according to Equations S1-S3.



$$K_{\text{rel}} = ([\mathbf{1}_2 \cdot \text{G2}][\text{G1}]) / ([\mathbf{1}_2 \cdot \text{G1}][\text{G2}]) \quad \text{— Eq. S4}$$

Scheme S1 shows the network of cross checking competition experiments that were carried out. For the series of five esters, all ten possible permutations were investigated. In addition, one pair was examined in both directions (a into b, then b into a). In each competition, the NMR spectrum was recorded both immediately and after 10 minutes to ensure equilibrium had been attained. The error in each measurement of K_{rel} was $\pm 5\%$.

The first set of competition experiments (Scheme S1 left) involved the addition of free ester **2**, **3**, **4** or **5** to a complex containing ester **6** (the arrow in the figure denotes which ester in each experiment was added to which complex). A subsequent set of competition experiments (Scheme S1 right), included: 1) reverse mixing, i.e., the addition of **6** to a complex of **2**, to ensure subtle solubility factors were insignificant; 2) cross-checks between different pairs of guests.



Scheme S1: Cross-checking network for determination of relative binding constants of esters **2-6** to host $\mathbf{1}_2$.

The same network of competition experiments was carried out with esters **7-11**, i.e., esters **7** through **10** were added to a complex of ester **11**. Likewise **7** added to a complex of **8**, **7** to **9**, **7** to **10**, **8** to **9**, **8** to **10**, **9** to **10**, and **11** to **7**. Two of the competition experiments, those involving **7/8**, and **7/9**, were found to attain equilibrium relatively more slowly than the others with equilibrium being established in 5 h.

¹H NMR Spectra of Selected Competition Experiments for Esters 2-7

Selected NMR spectra for the competition experiments of esters 2-7 are shown in Figures S13-S17. Integration of the resonances corresponding to the methyl groups of the two bound guests allowed determination of the concentration of the free guests and the two capsules.

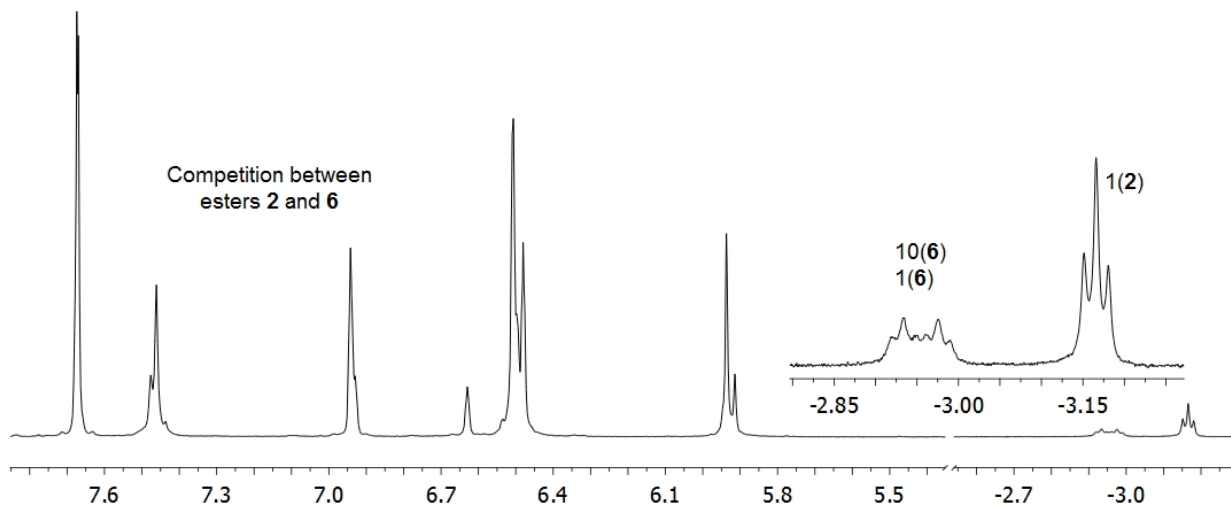


Figure S13: Competitive binding ¹H NMR spectrum between esters 2 and 6.

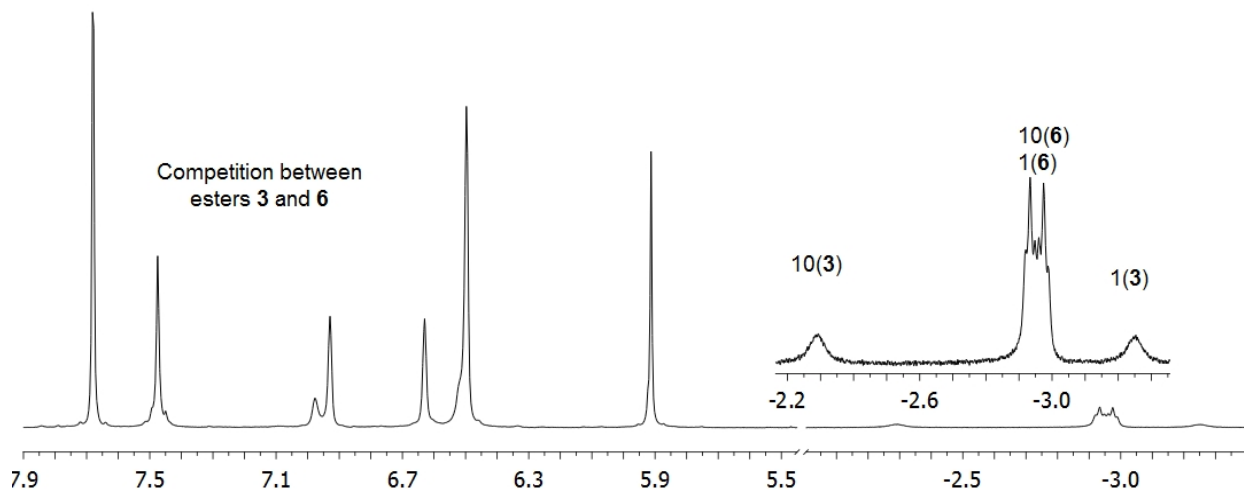


Figure S14: Competitive binding ¹H NMR spectrum between esters 3 and 6.

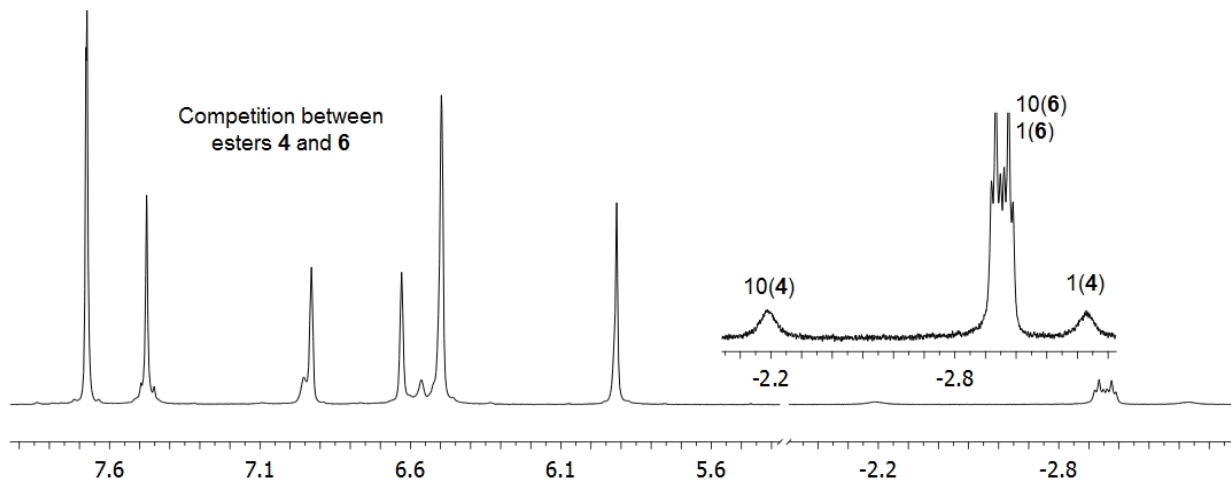


Figure S15: Competitive binding ^1H NMR spectrum between esters 4 and 6.

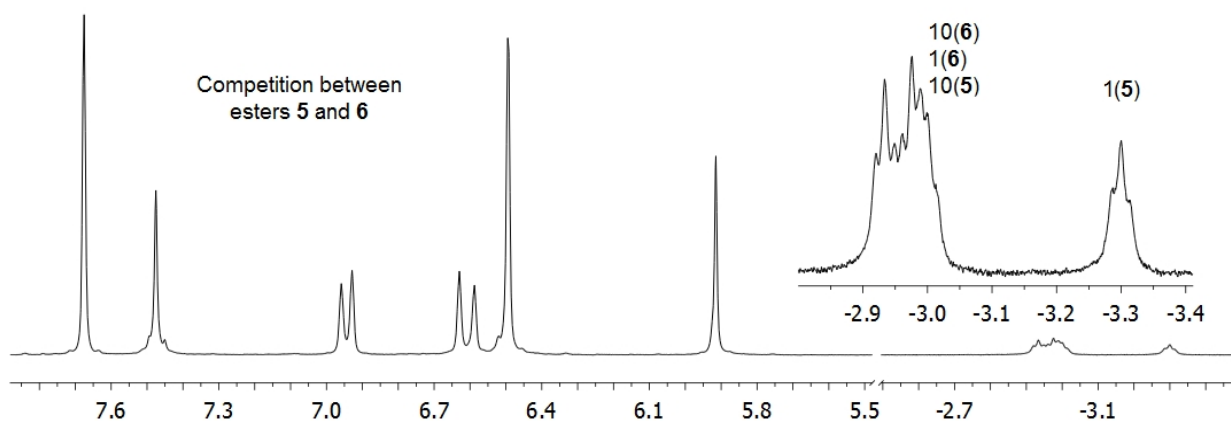


Figure S16: Competitive binding ^1H NMR spectrum between esters 5 and 6.

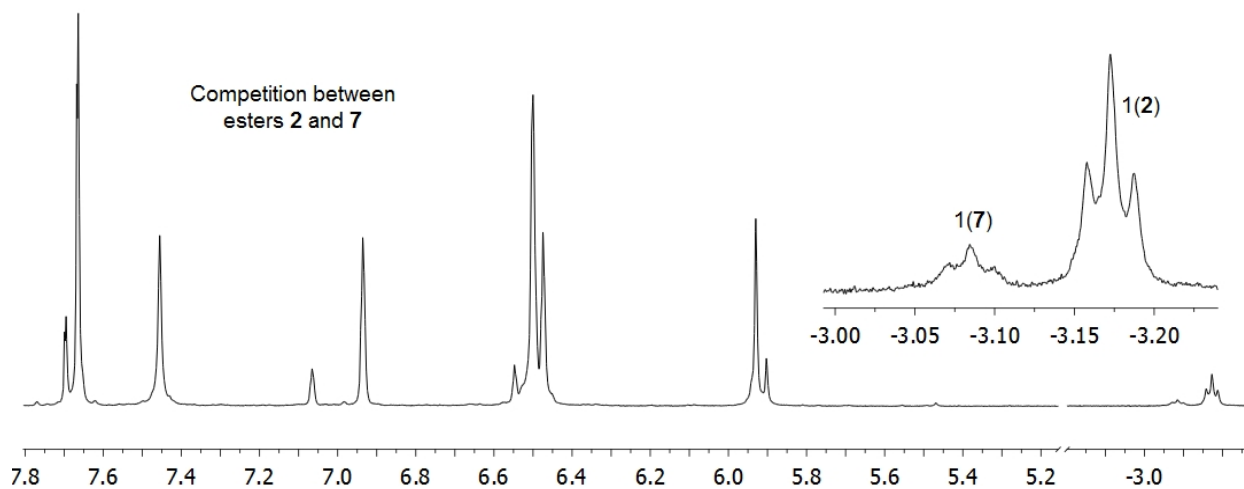


Figure S17: Competitive binding ^1H NMR spectrum between esters 2 and 7.

Relative Binding Constants of Esters 2-11

The relative binding constants of esters **2-11** are shown in Tables S2-S4. All differences are significant (error for individual K_{rel} determination was $\pm 5\%$). Data shown in Tables S2 and S3 were obtained directly from the aforementioned networks of competition experiments. The data shown in Table S4 was obtained by competition experiments between esters **7** with **5** (and **5** with **7**), and using this K_{rel} value and the experimentally derived values within each group to calculate the overall series of relative binding constants.

Table S2: Relative binding constants for Ester 2-6.

Esters	2	3	4	5	6
K_{rel}	165.4	1.8	1.0	10.7	16.4

Table S3: Relative binding constants for Ester 7-11.

Esters	7	8	9	10	11
K_{rel}	93.7	1.35	1.0	6.3	5.7

Table S4: Relative binding constants for Ester 2-11.

Esters	2	3	4	5	6	7	8	9	10	11
K_{rel}	1350	14.0	8.4	88.2	140.3	93.7	1.35	1.0	6.3	5.7

Hydrolysis of Free Esters

The hydrolysis rate constants of free esters **2-6** were obtained using ^1H NMR experiments and Origin 8.0 software. Integration of the $-\text{O}-\text{CH}_2$ group of the ester and the corresponding methylene group in the product alcohol gave the extent of hydrolysis as a function of time. The concentration of ester was 0.8 mM and the concentration of NaOH was 10 mM following pseudo-first order reaction conditions. The solvent, 3:7 acetone- d_6 : D_2O , was necessary to ensure homogeneity. Selected NMR spectra for the hydrolysis of free ester **6** are shown in Figure S18.

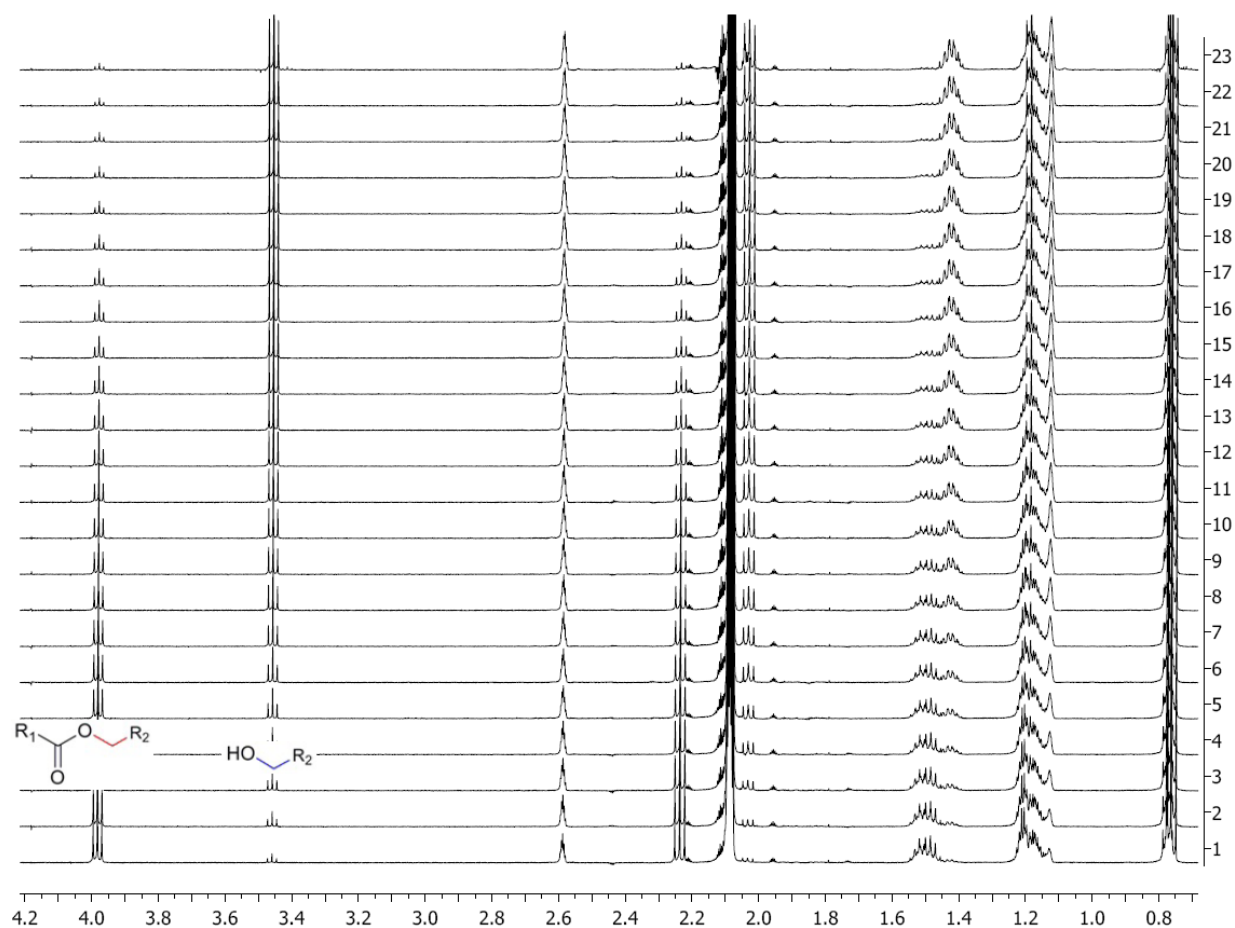


Figure S18: ^1H NMR spectra for the hydrolysis of free ester **6** at 20 °C (3:7 acetone- d_6 : D_2O ; [Ester **6**] = 0.8 mM; [NaOH] = 10 mM).

Rate Constants for the Hydrolysis of Esters 2-6

Hydrolysis data at 26 °C and curve fitting for free esters **2-6** are shown in Figure S19. Fitting was performed using Origin 8.0 (non-linear curve fit). All R^2 values are > 0.995 . Similar curves and fitting were obtained for each ester at 16 °C, 18 °C, 20 °C, 23 °C, 28 °C and 30 °C. The obtained hydrolysis rate constants (k_{obs}) of esters **2-6** at each temperature are shown in Table S5.

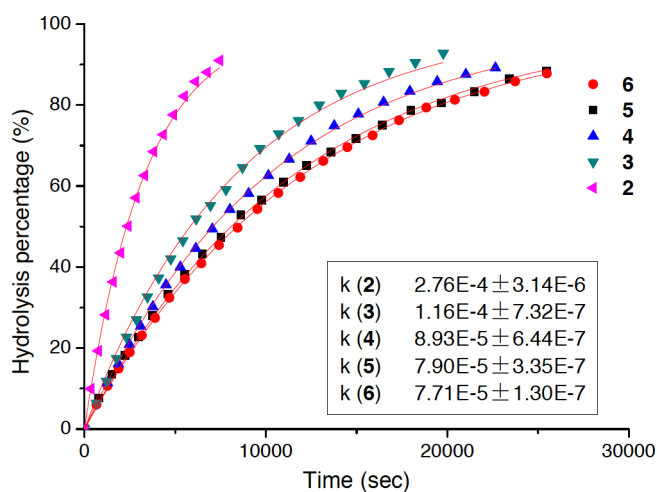


Figure S19: Fitting curves for the hydrolysis of esters **2-6** at 26 °C (3:7 acetone- d_6 : D_2O ; [Ester] = 0.8 mM; [NaOH] = 10 mM).

Table S5: Hydrolysis rate constants of esters **2-6** (pseudo-first order kinetics).

k_{obs} (s^{-1}) Ester	16°C	18°C	20°C	23°C	26°C	28°C	30°C
2	2.12E-04	2.44E-04	2.76E-04	3.35E-04	3.96E-04	4.43E-04	4.86E-04
3	8.99E-05	1.04E-04	1.16E-04	1.36E-04	1.63E-04	1.76E-04	2.00E-04
4	7.20E-05	7.99E-05	8.93E-05	1.03E-04	1.23E-04	1.38E-04	1.52E-04
5	6.23E-05	7.11E-05	7.90E-05	8.95E-05	1.06E-04	1.19E-04	1.30E-04
6	6.18E-05	6.97E-05	7.71E-05	8.85E-05	1.06E-04	1.17E-04	1.28E-04

Kinetic Resolution of Esters in the Presence of Host 1

Solutions were made such that the concentrations of the participating species were: Ester-a = Ester-b = 0.5 mM; Host = 1.0 mM; NaOD = 18.0 mM. Reactions were run in an NMR tube at 100 °C in a digital Dry-Bath Incubator (Fisher Scientific, model: 2001FS). At selected time intervals the tube was removed from the heating block and the reaction quenched by cooling the sample to room temperature using an ice-water mixture. Each reaction was monitored by NMR spectrometry until one ester had undergone complete hydrolysis (as judged by the bound guest methyl signals at ca. -3 ppm). The concentration of the slower reacting ester remaining was calculated by integration of the host 'd' peaks. The NMR spectrum of the resolution experiment with esters **2** and **4** at the point at which all of ester **4** had undergone hydrolysis (t = 17 min.) is shown in Figure S20. The outcome of the competition experiments between pairs of esters **2-6** is shown in Table S6.

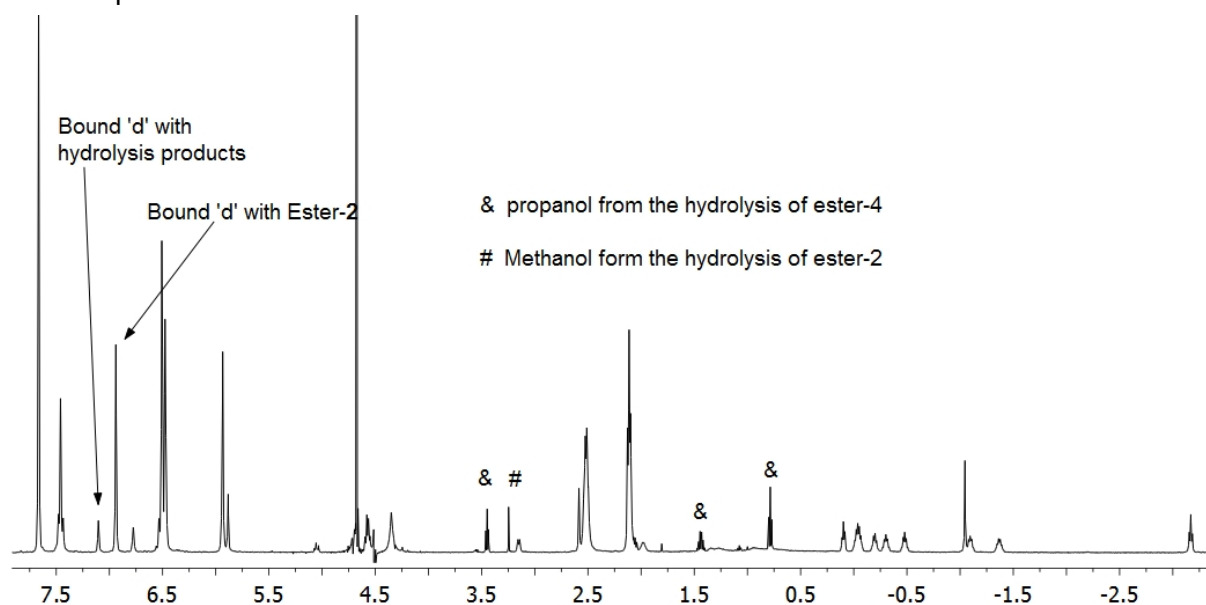


Figure S20: Recorded NMR of **2-4-1₂** (1:1:1) after 17 min. at 100 °C (18 mM NaOD).

Table S6: Outcome of competition experiments between pairs of esters **2-6**.

Ester	2	3	4	5	6
2	—				
3	82	—			
4	84	< 10	—		
5	46	44	52	—	
6	41	48	56	< 10	—

Note: Numerical values correspond to remaining percentage of slowly reacting ester (colored accordingly) when all of faster hydrolyzing ester had been consumed.

Hydrolysis of Individual Encapsulated Esters 2-6

The hydrolysis of each encapsulated esters **2-6** was performed under the following conditions: concentration of ester = 0.5 mM; host concentration = 1.0 mM; NaOH concentration = 18.0 mM, T = 100 °C. Several protocols were investigated, with the most efficient being that the reaction solution was partitioned between multiple NMR tubes that were placed in a digital Dry-Bath Incubator (Fisher Scientific, model: 2001FS). At selected time intervals a tube was removed from the heating block and the reaction quenched by placing the sample in a ice-water mixture. The extent of hydrolysis was then determined by NMR spectrometry. For each sample, the percentage of hydrolysis was calculated by the integration of the host 'd' peaks (~ 7 ppm) for the (dimeric) capsule containing the ester and the monomeric host containing carboxylate/alcohol products. By way of example, the recorded NMR spectra for the hydrolysis of ester **3** are shown in Figure S21.

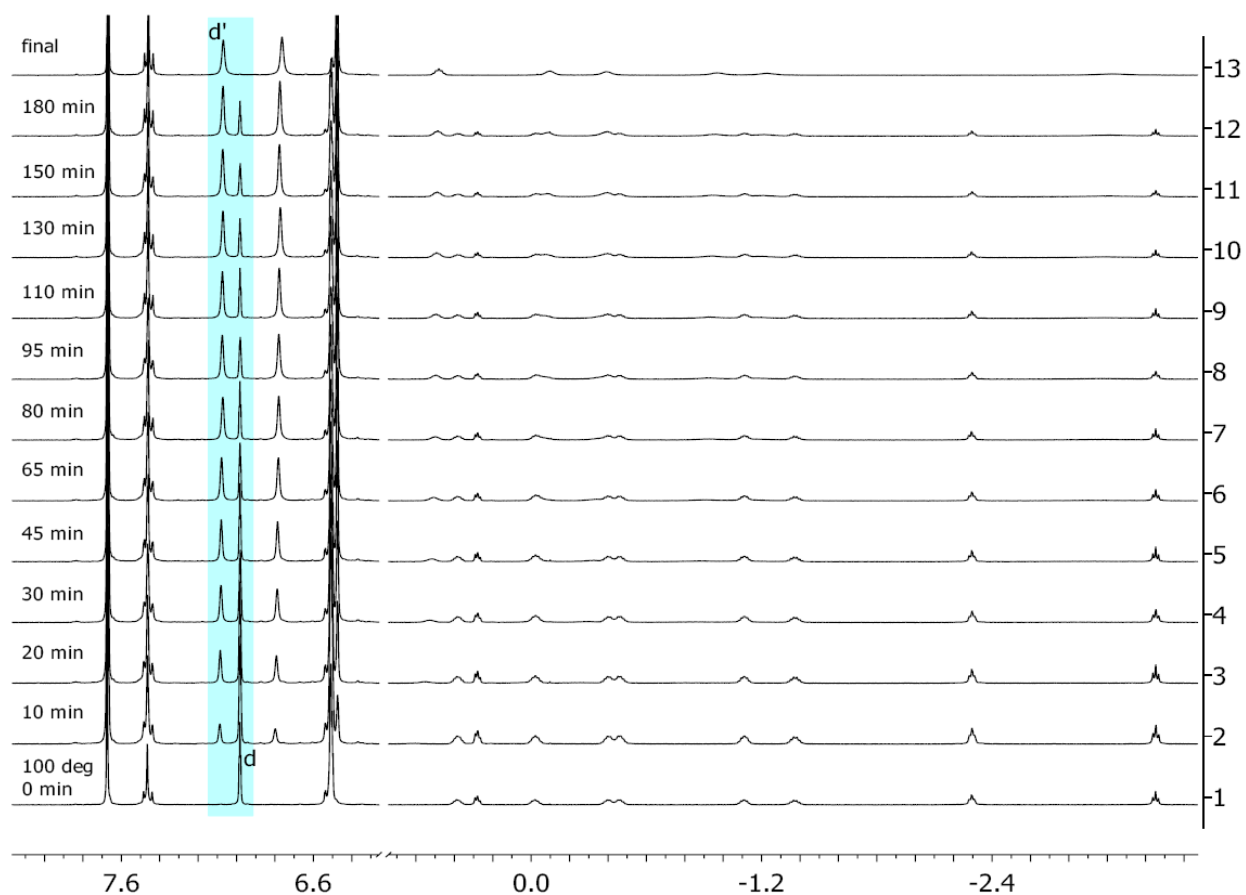


Figure S21: ^1H NMR stack for the hydrolysis of the complex formed between ester **3** and host **1₂** (1:1) at 100 °C in 18 mM NaOH.

Calculation of Rate Constants for Ester Hydrolysis at 100°C

The rate constants for ester hydrolysis at 100°C were determined by Arrhenius plots of the rate data obtained between 16°C and 30°C (see above). Thus, plots of $\ln k$ vs. $1/T$ gave k_{obs} at 100 °C, as well as the activation energy (E_a) and pre-exponential factor (A) for the hydrolysis of each ester (Figures S22-S26). Extrapolations to $1/T = 0$ (A), $1/T = 2.68 \times 10^{-3}$ (k_{obs} at 100 °C), the gradient (E_a) and the errors associated with each were calculated using Excel (LINEST). This data is presented in the main text (Table 1).

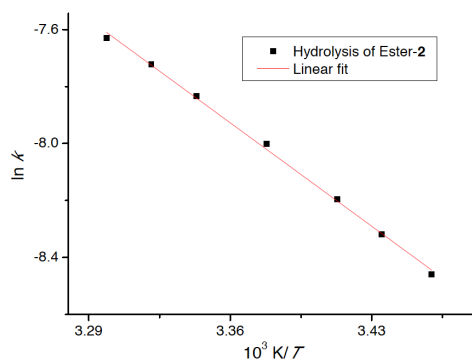


Figure S22: Arrhenius plot for the hydrolysis of ester 2.

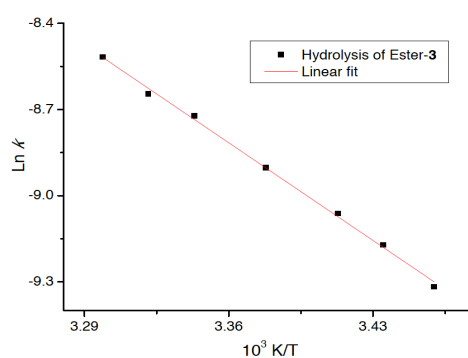


Figure S23: Arrhenius plot for the hydrolysis of ester 3.

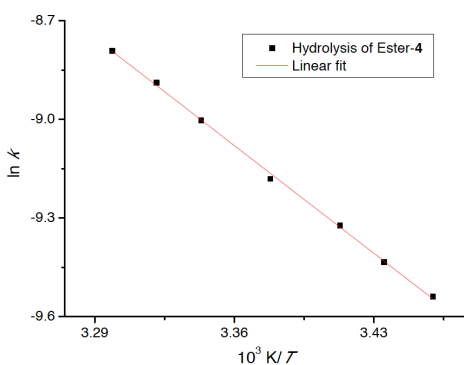


Figure S24: Arrhenius plot for the hydrolysis of ester 4.

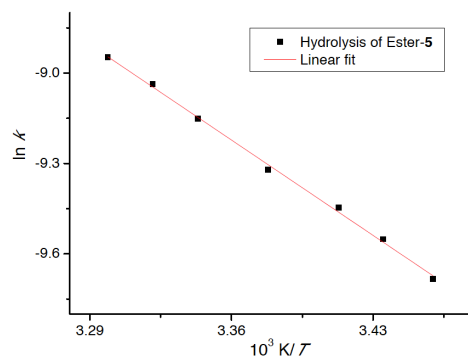


Figure S25: Arrhenius plot for the hydrolysis of ester 5.

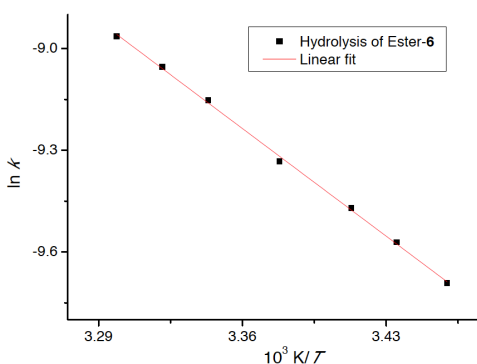
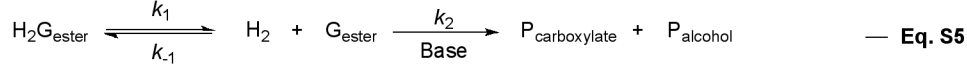


Figure S26: Arrhenius plot for the hydrolysis of ester 6.

Fitting for the Hydrolysis of Encapsulated Esters

The experimentally derived data for the hydrolysis of esters **2**, **3**, **4** and **6** in the presence of host **1** was fitted to the kinetic scheme defined by Equation S5. In this scheme, k_1 corresponds to the rate of dissociation of the ester from the capsule, k_{-1} is the corresponding rate of association, k_2 is the rate constant for reaction of the free ester at 100 °C, and k_{obs} is the observed rate constant for reaction of the free ester at 100 °C.



$$\frac{d[\text{P}_{\text{carboxylate}}]}{dt} = k_2[\text{G}_{\text{ester}}][\text{Base}] = k_{obs}[\text{G}] \quad \text{--- Eq. S6}$$

$$\frac{d[\text{G}_{\text{ester}}]}{dt} = k_1[\text{H}_2\text{G}_{\text{ester}}] - k_{-1}[\text{G}_{\text{ester}}][\text{H}_2] - k_2[\text{G}_{\text{ester}}][\text{Base}] \quad \text{--- Eq. S7}$$

Let $x = [\text{H}_2\text{G}_{\text{ester}}]$ and $y = [\text{G}_{\text{ester}}]$. Initially, at $T = 0$, both the total host, Host_2 , and guest, G_{ester} concentrations equal 0.5 mM and mass balance gives:

$$[\text{Host}_2]_{\text{total}} = x_t = [\text{H}_2\text{G}_{\text{ester}}] + [\text{H}_2]$$

and

$$[\text{G}_{\text{ester}}]_{\text{total}} = x_t = [\text{H}_2\text{G}_{\text{ester}}] + [\text{G}_{\text{ester}}]$$

where x_t equals 0.5 mM and so, initially, $[\text{G}_{\text{ester}}]$ equals $[\text{H}_2]$ or $y = x_t - x$. Assuming equilibrium, then the initial concentrations can be found from

$$K = k_1/k_{-1} = [\text{H}_2][\text{G}_{\text{ester}}]/[\text{H}_2\text{G}_{\text{ester}}] = (x_t - x)^2/x.$$

Solving for x , gives

$$x = x_t + K/2 - [(x_t + K/2)^2 - 4x_t^2]^{1/2}$$

and

$$y = K/2 + [(x_t + K/2)^2 - 4x_t^2]^{1/2}$$

As the hydrolysis proceeds, x and y change following Equation S7 and the rate equation for dissociation as

$$\begin{aligned} d[\text{G}_{\text{ester}}]/dt &= dy/dt = k_1 x + k_{-1} (x_t - x) y - k_{obs} y \\ d[\text{H}_2\text{G}_{\text{ester}}]/dt &= dx/dt = -k_1 x + k_{-1} (x_t - x) y. \end{aligned}$$

The two coupled differential equations are solved with the first order Euler method using a time step equal to 0.005 s. For each ester, a value for k_{obs} extrapolated from measured k_{obs} was used

and values for k_1 and k_{-1} were found which best fit the experimental hydrolysis data (see Figure 4 in main text). The calculated % hydrolysis curves show $[P_{\text{carboxylate}}]/x_t \times 100\%$ where, from mass balance, $[P_{\text{carboxylate}}] = x_t - x - y$.

The predicted k_1 , k_{-1} and association constants at 100 °C ($K_{a(100)} = k_1/k_{-1}$) are shown in Table S7. Also shown in Table 7 is the fit data (χ^2 and $\chi^2/\text{number of points}$) for each calculation. Graphical representations of each fit are shown in the main text (Figure 4).

Table S7: Fitting data for the hydrolysis of encapsulated esters at 100 °C.

Ester	k_1 ($\times 10^{-5} \text{ s}^{-1}$)	k_{-1} ($\text{s}^{-1} \text{ M}^{-1}$)	$K_{a(100)} = k_1/k_{-1}$ ($\times 10^3 \text{ M}^{-1}$)	Calculated k_{obs} at 373.15K ($\times 10^{-3} \text{ s}^{-1}$)	Chi²	Chi²/npts
2	13100.0	6.68×10^5	5102	12.2	111	9.25
3	10.7	1.24	11.6	4.03	169.6	11.3
4	12.8	2.14	16.7	2.75	41.6	4.16
6	2.3	0.68	29.4	2.13	29.9	2.72

Spiking the hydrolysis of an encapsulated ester with dodecane

In order to prove that hydrolysis occurs outside of capsule, and that the rate-determining step is the egression of the ester, the following experiment was performed. Two identical experiments were run in parallel in which the percent hydrolysis of encapsulated ester **4** was monitored. In one of these experiments, at $t = 40$ minutes the competitive guest dodecane was added. The NMR spectra of the respective samples at $t = 50$ and 60 minutes were subsequently recorded (Figure S27 shows the NMR spectra at $t = 50$ minutes). As the graph of time versus percentage hydrolysis shows, before spiking there was no discernable difference between the two (identical) experiments. However, the addition of dodecane caused all of the ester to rapidly undergo hydrolysis.

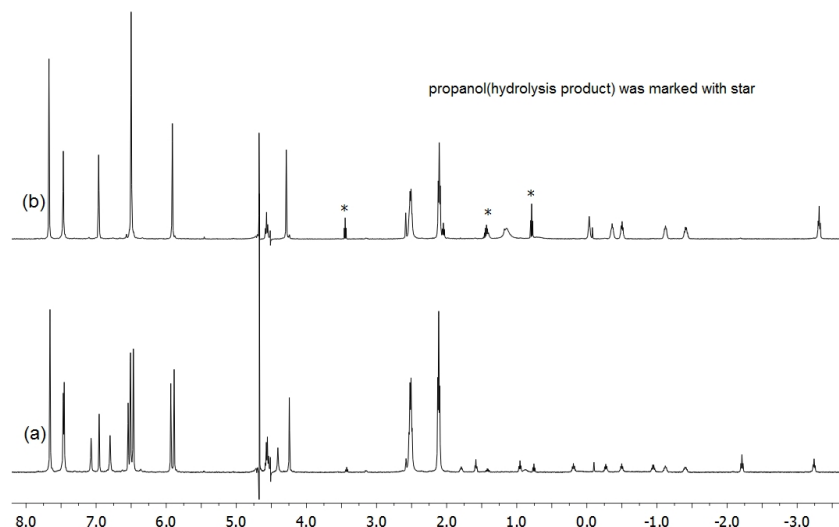


Figure S27: ^1H NMR of the hydrolysis of encapsulated **4**: a) $100\text{ }^\circ\text{C}$, $t = 50$ min.; (b) $100\text{ }^\circ\text{C}$, $t = 50$ min. upon spiking of complex with dodecane at $t = 40$ min.

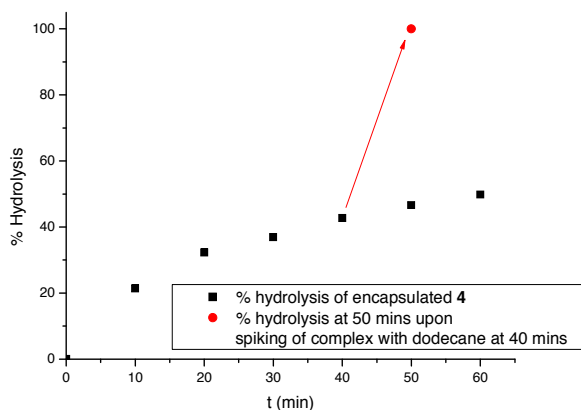


Figure S28: Hydrolysis of encapsulated **4** as a function of time.

The Complexation of the Hydrolysis Products to Host 1

By NMR titration and diffusion experiments it was observed that, with the exception of methanol, ethanol and propanol, all of the hydrolysis products form 1:1 complexes with host **1**. All complexations were fast exchanging on NMR time scale at room temperature. The diffusion constants (D_0) for each of those guests that form complexes are shown in Table S8. For comparison, the D_0 of free Host $\sim 1.75\text{E-}6$.² Figure S29 shows two NMR spectra for the titration of decanoic acid with host **1**.

Table S8: Diffusion constants of complexes of hydrolysis products with host.

Products	Butanol	Pentanol	Hexanoic acid	Heptanoic acid	Octanoic acid	Nonanoic acid	Decanoic acid
Binding mode	1 : 1	1 : 1	1 : 1	1 : 1	1 : 1	1 : 1	1 : 1
Diffusion constant (D_0 , $\text{cm}^2 \text{s}^{-1}$)	1.74E-6	1.75E-6	1.77E-6	1.76E-6	1.77E-6	1.75E-6	1.79E-6

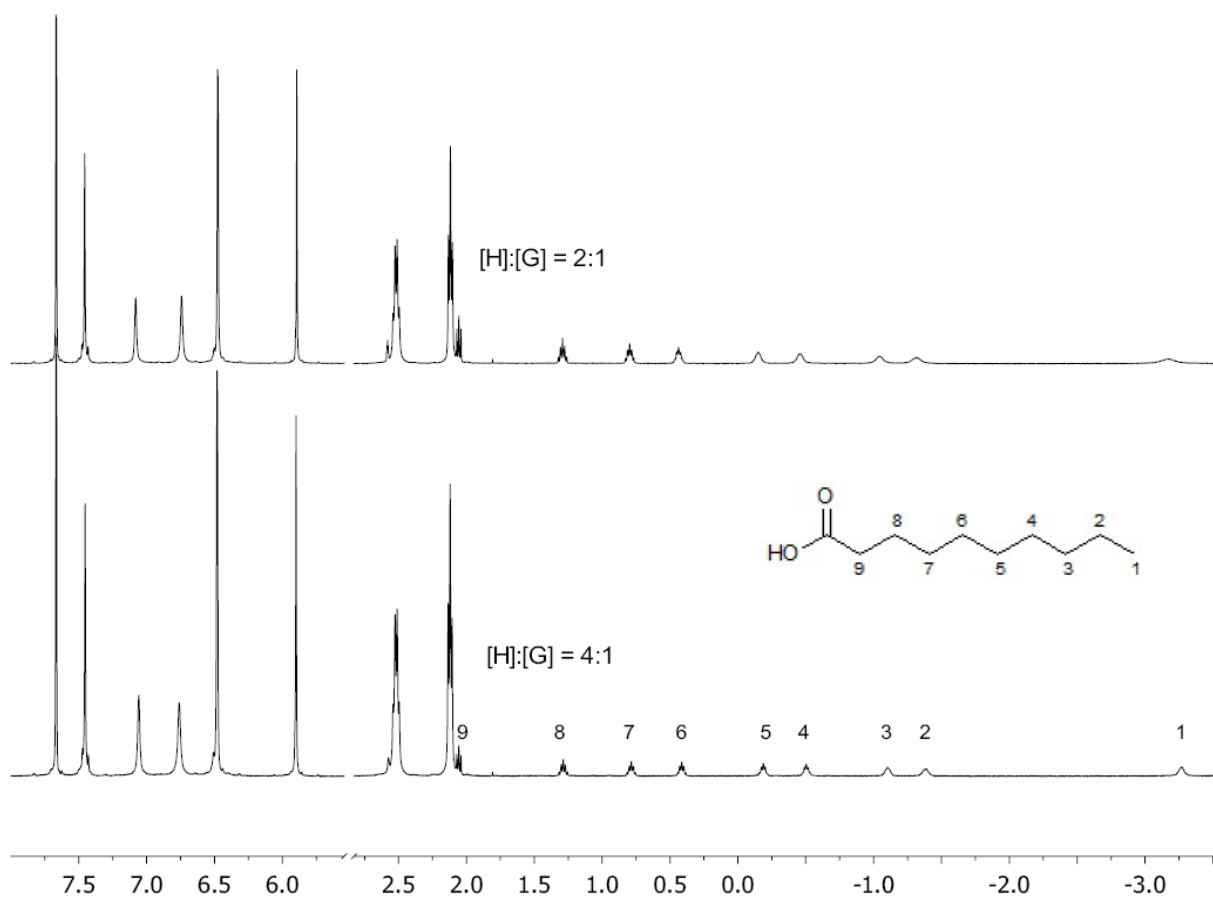


Figure S29: ¹H NMR for the binding of decanoic acid with host (fast exchange).

Competition Experiment Between Decanoic Acid and Ester 2

To confirm that the effect of product binding to host **1** minimally perturbs the kinetic model (Equation S5 above), a competition experiment between the strongest binding product, decanoic acid, and ester **2** was performed. From this experiment, a K_{rel} value of 1/40000 (relative to ester **2**) was determined. Figure S30 showed the NMR spectrum obtained in the competition between these two guests.

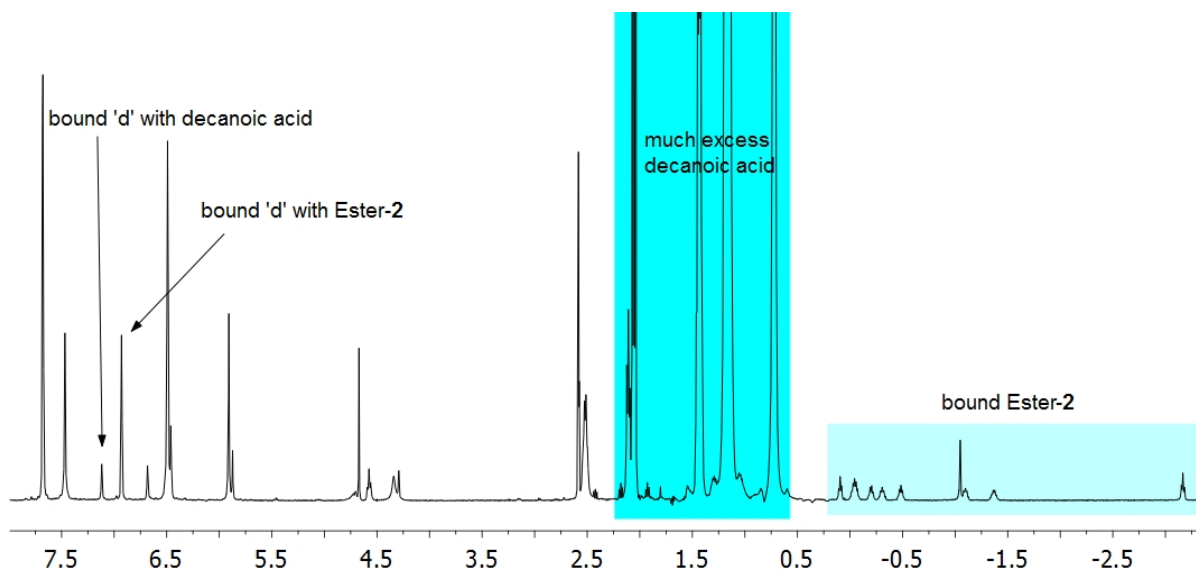


Figure S30: Competitive binding ¹H NMR spectrum between decanoic acid and ester **2** ([Host] = 0.56 mM; [Ester] = 0.28 mM; [decanoic acid] = 12.5 mM).

References

1. Gibb, C. L. D. & Gibb, B. C. Well Defined, Organic Nano-Environments in Water: The Hydrophobic Effect Drives a Capsular Assembly. *J. Am. Chem. Soc.* **126**, 11408-11409 (2004).
2. Gibb, C. L. D. & Gibb, B. C. Templated Assembly of Water-Soluble Nano-Capsules: Inter-Phase Sequestration, Storage, and Separation of Hydrocarbon Gases *J. Am. Chem. Soc.* **128**, 16498-16499 (2006).